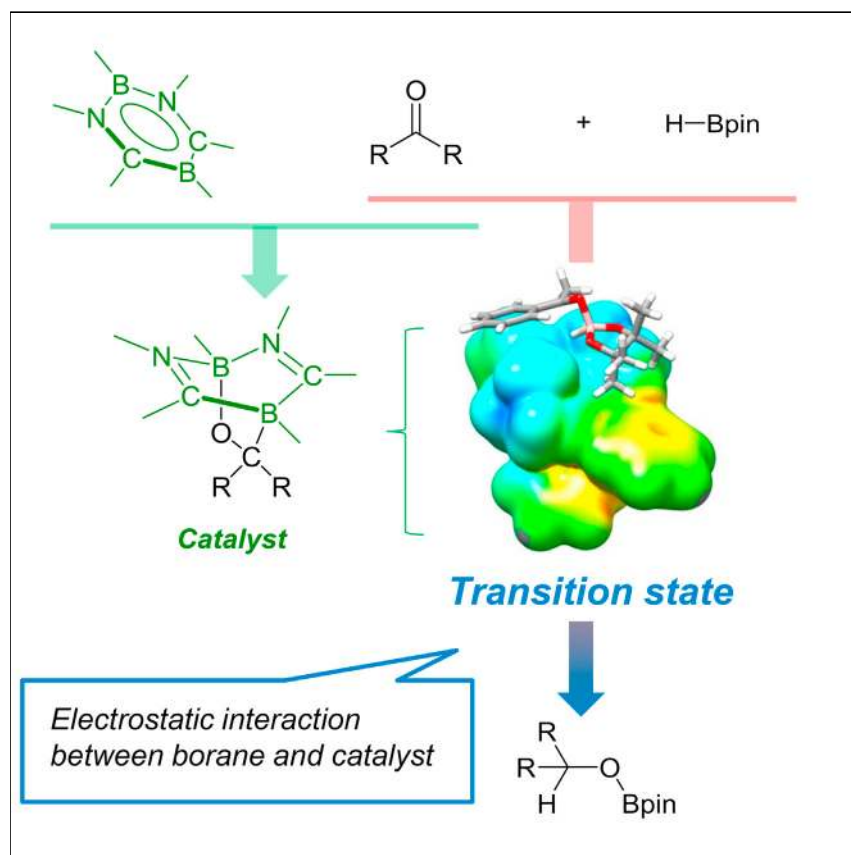


Article

Electrostatic Catalyst Generated from Diazadiborinine for Carbonyl Reduction



We show that, unlike other aromatic molecules, inorganic/organic hybrid benzene, namely diazadiborinine, effectively accelerates hydroboration of carbonyl derivatives. Experimental mechanistic investigations indicate that the adduct of diazadiborinine with a carbonyl derivative formed at the initial step of the reaction serves as the actual active catalyst. Computational studies suggest that the transition state is stabilized by an electrostatic effect.

Di Wu, Ruixing Wang, Yongxin Li, Rakesh Ganguly, Hajime Hirao, Rei Kinjo

hhirao@cityu.edu.hk (H.H.)
rkinjo@ntu.edu.sg (R.K.)

HIGHLIGHTS

Aromatic diazadiborinine promotes catalytic hydroboration of carbonyls

Actual catalyst is the adduct of diazadiborinine with carbonyl derivatives

Mechanism involves a transition state stabilized mainly by an electrostatic effect



Article

Electrostatic Catalyst Generated from Diazadiborinine for Carbonyl Reduction

Di Wu,¹ Ruixing Wang,² Yongxin Li,³ Rakesh Ganguly,³ Hajime Hirao,^{1,2,*} and Rei Kinjo^{1,4,*}

SUMMARY

Since the seminal discovery by van der Waals in the late 19th century that weak attractive forces exist between even electrically neutral atoms or molecules, a number of noncovalent interactions have been recognized. Among them, electrostatic interactions such as hydrogen bonds play pivotal roles in countless chemical processes and biochemical living systems. By mimicking biocatalysis, various organocatalysts equipped with hydrogen-bond functionality have been developed; however, a challenge has persisted in designing catalysts exploiting other types of noncovalent interactions. Here, we report metal-free hydroboration reactions of carbonyl compounds and CO₂ catalyzed by aromatic diazadiborinine. A joint experimental and computational study on the reaction mechanism suggests that adducts of diazadiborinine with carbonyl and CO₂ formed at the initial stage of the reactions serve as actual catalysts. The former stabilizes the transition state by using the electrostatic interaction between the hydride of borane and the polar, hole-shaped structure of the adduct.

INTRODUCTION

Noncovalent interactions such as hydrogen bonding, halogen bonding, π - π stacking, and ion/lone pair π interactions, are ubiquitously involved in a myriad of chemical transformation processes.^{1–5} Notably, such interactions contribute significantly to catalytic processes found in nature. For instance, enzymes use hydrogen bonding as one of the major catalytic factors that stabilize transition states, thereby facilitating chemical transformations of substrates.^{6–8} By mimicking enzymatic biocatalysis, diverse small-molecule catalysts that exploit hydrogen bonds have emerged over the past several decades.^{9–14} However, the development of catalysts relying on electrostatic effects other than hydrogen bonding still remains challenging.^{15–19}

Carbonyl reductions are useful methodologies for the synthesis of various products and hence have been extensively used in organic syntheses and industrial processes.^{20–24} Among them, hydroboration has attracted considerable attention, because boron hydrides are relatively stable and can easily be stored, which circumvents the drawbacks of the use of highly flammable and highly pressurized hydrogen gas.^{25–30} In addition, the resulting boric and borinic esters serve as versatile synthetic intermediates for the preparation of a wide range of chemicals and materials.^{31–33} In this regard, a variety of transition-metal complexes capable of promoting hydroboration of carbonyl derivatives have been developed over the past two decades.³⁴ By contrast, despite recent advances in main-group chemistry made with these elements as alternatives to transition metals,^{35–37} catalytic hydroboration reactions that operate with well-defined main-group catalysts are still

The Bigger Picture

Noncovalent interactions are ubiquitously used for chemical transformations in nature. For instance, one of the major catalytic factors of enzymes is the electrostatic effect that stabilizes transition states. By mimicking geometric and electronic structures of enzymes, small organic molecules featuring similar functionality to enzymes can be produced. This work presents metal-free catalytic hydroboration of carbonyl compounds promoted by aromatic diazadiborinine. In stark contrast to the reaction pathways proposed for catalytic hydroboration with other main-group catalysts, the mechanism for the reaction reported here does not involve bond formation or dissociation between the catalyst and substrate. The computational analysis provides a rationale for the catalytic action, in which a low-energy pathway is achieved by an electrostatic effect.

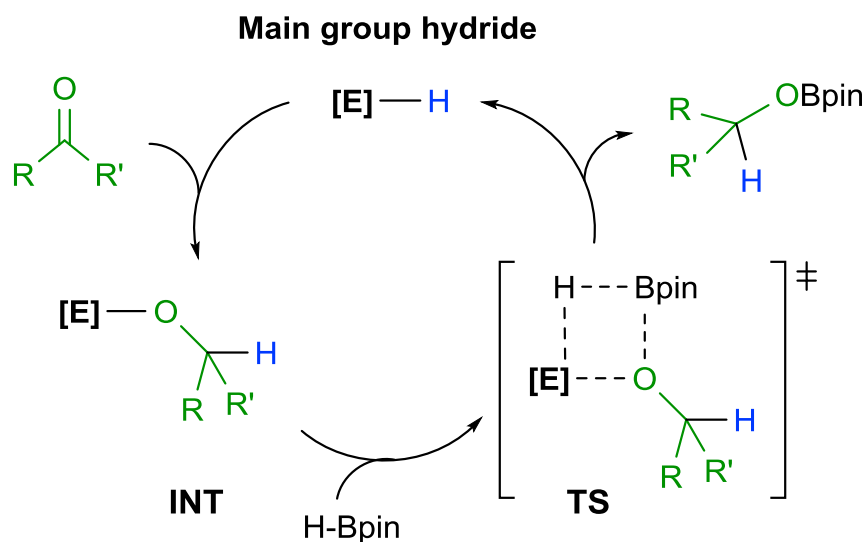


Figure 1. Catalytic Cycles for Hydroboration of Carbonyls with Main-Group Catalysts

Commonly proposed hydride insertion \rightarrow σ -bond metathesis pathway for catalytic hydroboration reactions with main-group hydride catalysts ([E] = Mg, Ge, Sn, Al, B, P).

limited, and in particular, the metal-free catalytic system remains virtually unexplored.^{38,39} Thus far, main-group metal catalysts based on Mg,^{40–45} Ge(II) and Sn(II),^{46–50} Al,^{51,52} and alkali metal borates⁵³ have been reported, whereas our group has demonstrated that even nonmetal 1,3,2-diazaphospholene can be used as a catalyst for hydroboration of carbonyl compounds.⁵⁴ Remarkably, irrespective of the main-group element involved, a common reaction pathway for hydroboration is proposed involving the following steps (Figure 1): (1) insertion of the C=O bond of a carbonyl compound into the [E]–H bond of main-group catalysts to generate intermediate INT, (2) interaction between INT and HBpin to form four-membered transition state TS, and (3) formation of the hydroboration product via σ -bond metathesis. As far as we are aware, a main-group catalytic system based on a mechanism other than the insertion-metathesis pathway has never been described.

Recently, we have reported the isolation of aromatic diazadiborinine derivatives **1a** and **1b** (Figure 2A) and have shown that the two boron centers in these molecules cooperatively activate unsaturated substrates such as alkynes and alkenes.^{55–57} For instance, **1c** can be obtained from the reaction of **1a** with ethylene. Although these findings demonstrate the potential of B,N-cyclic molecules for broad applications,^{58–60} to the best of our knowledge, aromatic six-membered B,N-heterocycles have never been used as promoters for catalytic reactions.^{61,62} Here, we report diazadiborinine-catalyzed hydroboration of carbonyl derivatives as well as N-formylation of amines with the use of CO₂ under ambient conditions. We demonstrate that different pathways are used for these catalytic reactions, one of which exploits a unique electrostatic effect.

RESULTS AND DISCUSSION

Catalytic Hydroboration of Ketones and Aldehydes

Our preliminary studies showed that **1b** activates both unsaturated bonds and E–H σ bonds (E = B, Si, P), whereas **1a** reacts only with unsaturated bonds at ambient condition (see below), which prompted us to use **1a** as the catalyst for the investigation of catalytic hydroboration. Initial assessments of the catalytic activity of **1a** were

¹Division of Chemistry and Biological Chemistry, School of Physical and Mathematical Sciences, Nanyang Technological University, 21 Nanyang Link, 637371 Singapore, Singapore

²Department of Biology and Chemistry, City University of Hong Kong, Tat Chee Avenue, Kowloon, Hong Kong, China

³NTU-CBC Crystallography Facility, Nanyang Technological University, 21 Nanyang Link, 637371 Singapore, Singapore

⁴Lead Contact

*Correspondence: hhirao@cityu.edu.hk (H.H.), rkinjo@ntu.edu.sg (R.K.)

<http://dx.doi.org/10.1016/j.chempr.2017.06.001>

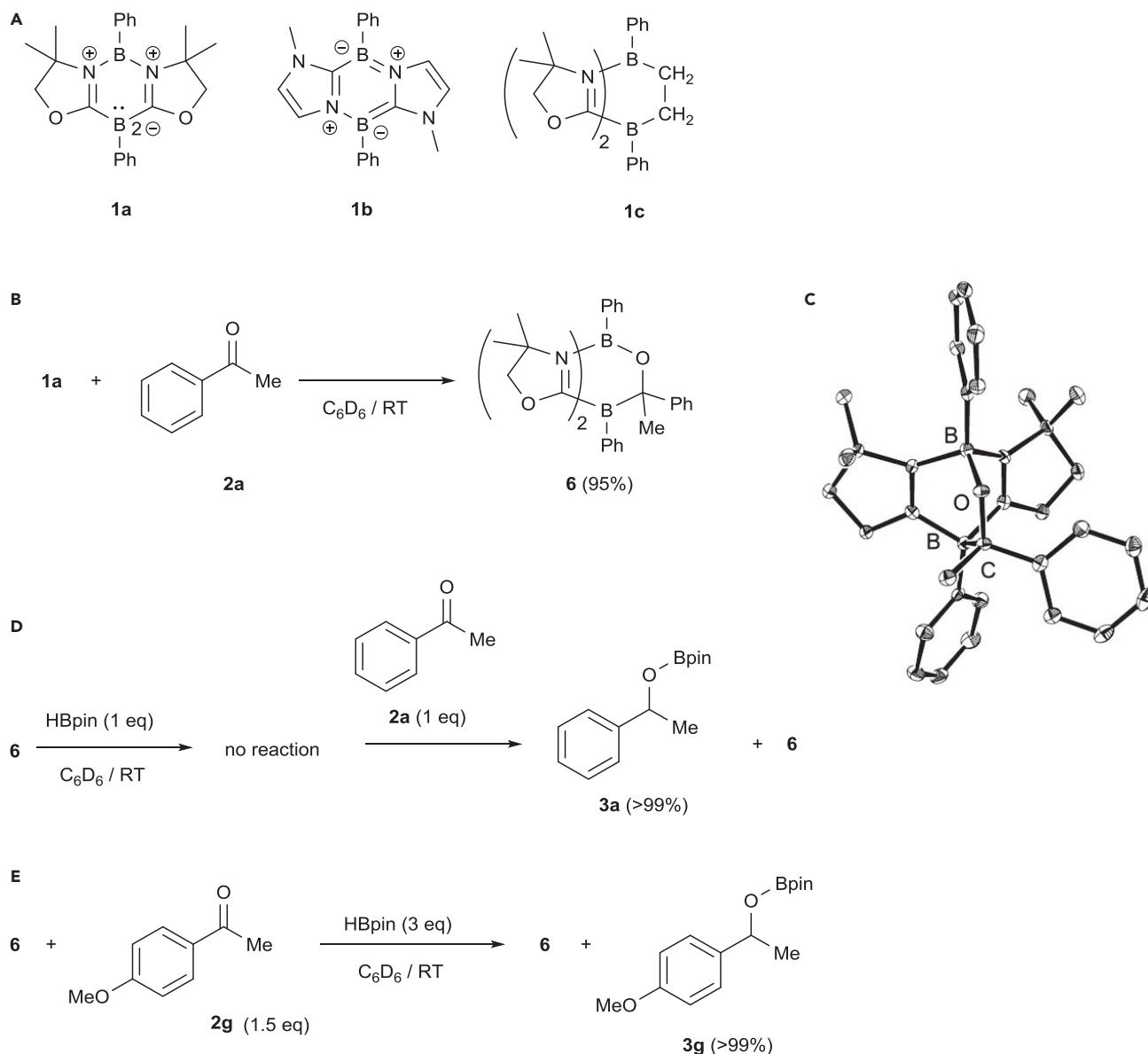


Figure 2. Schematic Representation of Diazadiborinine Derivatives and Their Reactivity

(A) 1,3,2,5-Diazadiborinine **1a**, 1,4,2,5-diazadiborinine **1b**, and **1a**-ethylene adduct **1c**.

(B) Synthesis of **6**.

(C) Solid-state structure of **6**.

(D) Reaction of **6** with HBpin and **2a**.

(E) Reaction of **2g** and HBpin in the presence of **6**.

undertaken for the reduction of acetophenone **2a** (Table 1). At first, the control experiment confirmed that no reaction between acetophenone and HBpin proceeded in the absence of **1a** (entry 1). With 5 mol % of **1a**, acetophenone **2a** was fully converted to the corresponding borinic ester PhMeHC-OBpin **3a** after 2 hr (entry 2). When the catalyst loading was decreased to 2 mol %, the borinic ester **3a** was still obtained quantitatively within 2 hr (entry 3), whereas further reduction of the catalyst loading to 1 mol % required longer reaction time (entry 4). Interestingly, the reaction in CD₃CN was completed within 30 min (entry 5). When 9-borabicyclo[3.3.1]nonane (9-BBN) was used, borinic ester **3a'** was formed in excellent yield after 6.5 hr (entry 6).

Table 1. Optimization of the Reaction Conditions

Entry	Catalyst (mol %)	Borane (1.0 equiv)	Solvent	Time (hr)	Yield (%) ^a
1	0	HBpin	C ₆ D ₆	2	0
2	5	HBpin	C ₆ D ₆	2	95
3	2	HBpin	C ₆ D ₆	2	98
4	1	HBpin	C ₆ D ₆	8	98
5	2	HBpin	CD ₃ CN	0.5	98
6	2	9-BBN	C ₆ D ₆	6.5	98

Reaction conditions: acetophenone (0.269 mmol), H source (0.269 mmol), solvent (0.5 mL).

^aYields were determined by ¹H NMR spectroscopy using 1,3,5-trimethoxybenzene as an internal standard.

The use of triethoxysilane ((EtO)₃SiH) did not afford the corresponding hydrosilylation products (see [Supplemental Information](#) and [Figure S1](#)). Note that the result presents a rare example of metal-free organoboron-catalyzed hydroboration of carbonyl derivatives.

With the optimized reaction conditions in hand, the scope of the catalytic reaction was briefly examined with the use of various ketones ([Table 2](#)). Aliphatic ketones **2b–2e** afforded the corresponding boric esters **3b–3e** in excellent yields. Ketone derivatives **2f–2j** involving electron-withdrawing as well as electron-donating aromatic groups were well tolerated. When α,β -unsaturated ketones **2k** and **2l** were used, hydroboration occurred selectively only at the carbonyl functional groups. Benzoquinone **2m** furnished 1,4-(pinBO)₂C₆H₄ **3m**. The scope of the reaction was further studied with aldehyde substrates ([Table 3](#)). Both aliphatic and aromatic aldehydes **4a–4h** afforded the corresponding boric esters **5a–5h** nearly quantitatively. With 2 equiv of HBpin, hydroboration of terephthalaldehyde **4i** proceeded smoothly and bis-boric ester **5i** was gained in excellent yield. Although a longer reaction time was required, a similar process was observed for 4-acetylbenzaldehyde **4j**, which afforded **5j**.

To gain insight into the reaction mechanism, we performed several control reactions in a stoichiometric manner. Although compound **1a** did not react with HBpin, **1a** cleanly underwent [4 + 2] cycloaddition with acetophenone **2a**, and the corresponding bicyclo[2.2.2] derivative **6** was obtained in 95% isolated yield ([Figure 2B](#)). Compound **6** was fully characterized by standard spectroscopic methods and X-ray diffraction analysis ([Figure 2C](#)). The formation of **6** via a regioselective [4 + 2] cycloaddition is in line with our previous observation for **1a**. Thus, the B atom between two carbon atoms serves as a Lewis basic center, whereas the B atom between two N atoms acts as a Lewis acidic center.^{55,56} We also confirmed that retro-[4 + 2] cycloaddition of **6** did not take place even at 70°C. Surprisingly, compound **6** did not react with HBpin ([Figure S2](#)). Addition of acetophenone **2a** to a C₆D₆ solution of a mixture of **6** and HBpin afforded product **3a** at ambient conditions ([Figure 2D](#)). These observations suggest that dissociation of the PhMeCO fragment from **6** concomitant with the regeneration of **1a** is not involved in the reaction to produce **3a**. To confirm this hypothesis, we performed a further reaction ([Figure 2E](#)). To the mixture of **6** and

Table 2. Scope of Catalytic Hydroboration of Ketones

2	Time	Product 3	Yield (%) ^a	TON	TOF (hr ⁻¹) ^b
2b	2.75 hr	3b	98	49	18
2c	168 hr	3c	85	43	0.3
2d	<10 min	3d	98	49	>288 ^c
2e	2-adamantanone	3e	98	49	>288 ^c
2f		3f	98	49	25
2g		3g	95	48	1
2h		3h	98	49	20
2i ^d		3i	98	49	16
2j ^d		3j	96	48	6
2k		3k	98	49	5
2l		3l	98	49	16
2m ^e		3m	98	49	>288 ^c

^aYields were determined by ¹H NMR spectroscopy using 1,3,5-trimethoxybenzene as an internal standard.

^bTurnover frequency (TOF) = turnover number (TON)/average reaction time.

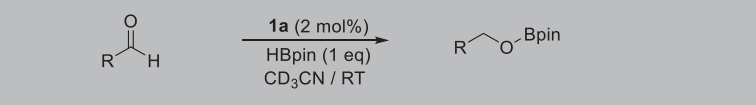
^cTOF lower limit.

^dReaction conducted with C₆D₆ as solvent.

^eHBpin (2 equiv) was used in this reaction.

4'-methoxyacetophenone **2g** in C₆D₆, 3 equiv of HBpin was added, and the reaction was monitored by NMR spectroscopy. Within 50 min, full conversion of **2g** to **3g** was observed without formation of a trace amount of **3a** (Figure S4). We also confirmed that compound **6** remained unchanged during the reaction, which led us to

Table 3. Scope of Catalytic Hydroboration of Aldehydes

					
4	Time	Product 5	Yield (%) ^a	TON	TOF (hr ⁻¹) ^b
4a	1.83 hr	5a	98	49	27
4b	<10 min	5b	98	49	>288 ^c
4c	15 min	5c	98	49	196
4d	<10 min	5d	98	49	>288 ^c
4e	<10 min	5e	98	49	>288 ^c
4f	20 min	5f	98	49	148
4g	50 min	5g	98	49	59
4h	7 hr	5h	98	49	7
4i ^d	1 hr	5i	98	49	49
4j ^d	168 hr	5j	57	29	0.2

^aYields were determined by ¹H NMR spectroscopy using 1,3,5-trimethoxybenzene as an internal standard.

^bTurnover frequency (TOF) = turnover number (TON)/average reaction time.

^cTOF lower limit.

^dHBpin (2 equiv) was used in this reaction.

postulate that **6** is the true active catalyst rather than the resting state in the hydroboration reaction.

Kinetic Study

To better understand the reaction pathway, we carried out further analysis of the catalytic reaction. C₆D₆ solutions of various concentrations of **1a**, HBpin, and

diisopropyl ketone **2c** were prepared in a sealed NMR tube, and the reactions were monitored at room temperature by ^1H NMR at 2-min intervals. On the basis of the rate constants k_{obs} simulated from the kinetic conversion charts (see the [Supplemental Information](#)), we determined the rate law, which can be represented by $k_{\text{obs}} = k[1\mathbf{a}]^1[\text{HBpin}]^1[2\mathbf{c}]^1$. An Eyring plot was constructed for kinetic data obtained at 10°C intervals from 35°C to 65°C, and activation parameters extracted from the Eyring analysis yielded values of $\Delta H^\ddagger = 8.6 \pm 1.0 \text{ kcal mol}^{-1}$, $\Delta S^\ddagger = -50.7 \pm 3.1 \text{ e.u.}$, and $\Delta G^\ddagger(298) = 23.7 \pm 1.9 \text{ kcal mol}^{-1}$. The large negative ΔS^\ddagger is in line with the high molecularity of the rate law. Next, deuterated kinetic isotope effects (DKIEs) on the reactions with diisopropyl ketone **2c** were investigated with deuterated pinacolborane (DBpin). To a C_6D_6 solution of diisopropyl ketone **2c** with 3 mol % of **1a**, excess amounts of deuterated pinacolborane (5.1 equiv) were added at room temperature, and the reaction was monitored by NMR every 10 min. The DKIE value was estimated on the basis of the rate constants, and a DKIE of 3.65 was obtained for the reactions. We also performed the same reaction with ^{18}O -labeled diisopropyl ketone **2c**- ^{18}O , for which a $^{16}\text{O}/^{18}\text{O}$ KIE value of 1.83 was determined.^{63,64} The double KIE reaction using both DBpin and **2c**- ^{18}O provided the largest DKIE of 5.97, thus suggesting that the rate-determining step could involve the dissociation of the B–H bond in HBpin and the C=O bond in **2c** and/or the formation of B–O and C–H bonds.

DFT Study for the Reaction Profile of Hydroboration

Pathways for the reaction of acetophenone (**2a**) with pinacolborane (HBpin), catalyzed by **6**, were explored theoretically by density functional theory (DFT) calculations at the M06-2X(SCRF)/def2-TZVP//M06-2X(SCRF)/6-31G* level. The solvent effect of acetonitrile was described by the SCRF (IEFPCM) solvent model. An energetically feasible reaction pathway was obtained and is depicted in [Figure 3A](#). The barrier for this pathway via TS was calculated as $27.1 \text{ kcal mol}^{-1}$, which is reasonably low and the lowest of all the barriers obtained ([Figure S46](#)). Interestingly, no intramolecular bond dissociation/recombination of **6** is involved in this path. Instead, compound **6** cuddles up to the migrating hydride and assists a direct insertion of the B–H bond of HBpin into the C=O moiety of **2a** at the transition state. [Figure 3B](#) (left and middle) illustrates an electrostatic potential map at the transition state in which the electrostatically positive and hole-shaped site of **6** interacts with the negatively charged hydride of HBpin. Thus, **6** can be viewed as an electrostatic catalyst possessing a B–H hydride hole. The key interatomic distances at the transition state ([Figure 3B](#), right) confirm that the hydride of HBpin is surrounded by the hydrogen atoms carrying partial positive charges (highlighted in yellow; see [Figure S47](#)). In this transition state, which corresponds to the rate-determining step of this reaction, both the cleavage of the B–H and C=O bonds and the formation of the B–O and C–H bonds are involved, which is therefore consistent with the result of double KIE analysis. Note that the optimized structure of the transition state in the reaction with 9-BBN is essentially identical to that obtained with HBpin ([Figure S48](#)). Other reaction pathways that use the B–O–C–B moiety of **6** as the active site were found to have much higher barriers ([Figure S46](#)), which indicates that these processes are unlikely to occur.

Catalytic Hydroboration with **1c** and Related Molecules

To further prove the catalytic mechanism based on electrostatic interaction and to confirm the innocence of the B–O–C–B moiety of the **1a**-carbonyl adducts in the catalytic process, we carried out a catalytic reaction by using **1c**. First, we confirmed that there was no conversion of **1c** to **6** in a C_6D_6 solution even in the presence of **2a** (1.0 equiv) ([Figure S28](#)). A CD_3CN solution of **2a** and HBpin (3 equiv) in the presence

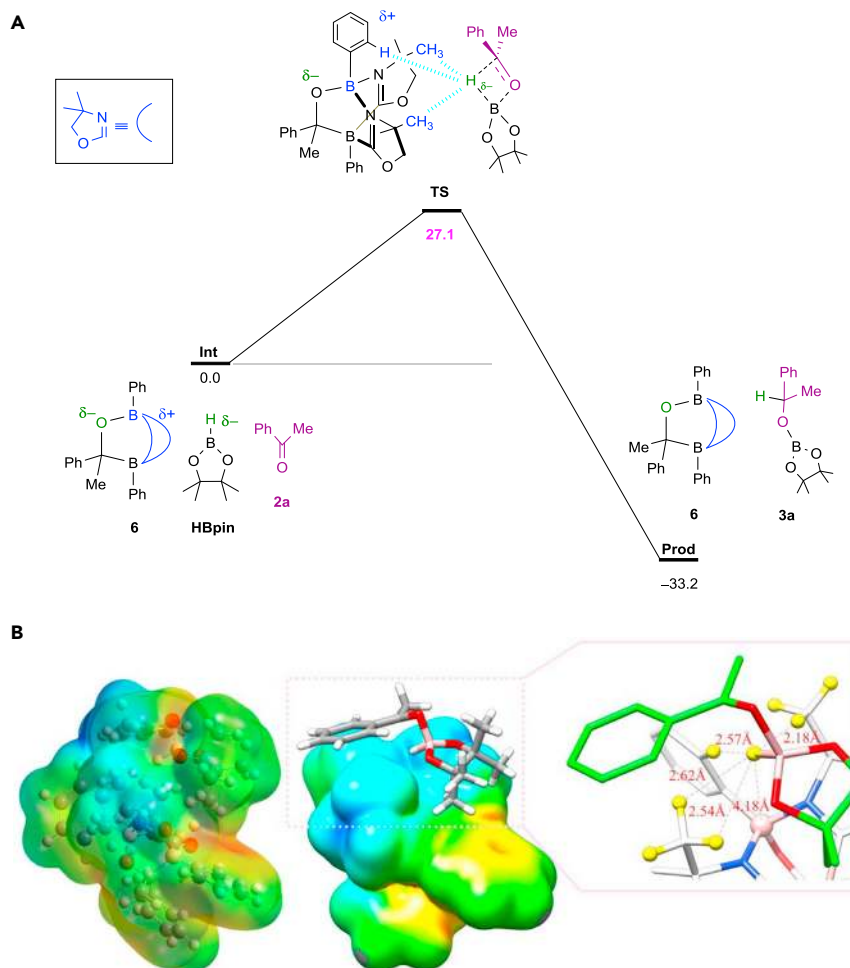


Figure 3. DFT-Calculated Free-Energy Profile of a Plausible Mechanism

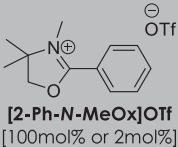
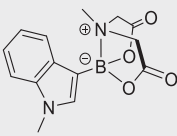
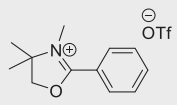
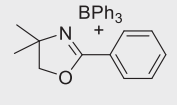
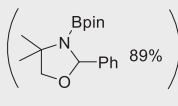
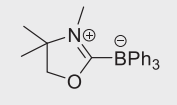
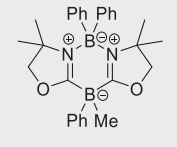
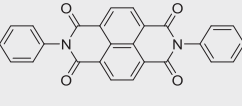
(A) Free-energy profile (in kcal mol⁻¹) for the reaction between 2a and HBpin catalyzed by 6 in CH₃CN at 298 K, as determined at the M06-2X(SCRF)/def2-TZVP//M06-2X(SCRF)/6-31G* level of theory.

(B) Electrostatic potential map for the transition state.

of 2 mol % of 1c was prepared in a sealed NMR tube, and the reaction was monitored by NMR spectroscopy. After 10 hr at room temperature, nearly quantitative formation of 3a was confirmed (Figures S29 and S30). With 2h under the same conditions, 3h was obtained in 93% yield after 21 hr (Figures S31 and S32). These observations demonstrate that the B–O–C–B moiety of 1a-carbonyl adducts does not serve as an active site during the hydroboration reactions with 1a as pre-catalysts. Compared with the reaction with 1a (Table 2), longer reaction periods were required with the 1c catalyst for the quantitative formation of 3a and 3h, which is probably as result of the less polar nature of 1c with respect to 1a-carbonyl adducts. Thus, a more polar catalyst could stabilize the transition state more effectively, which is in line with the computational result. In fact, the sum of natural population analysis charge (+0.65) for the 1a fragment in 6 is found to be larger than that (+0.39) for the corresponding moiety in 1c.

The electrostatic interaction is different from the charge-transfer interaction via orbital interactions but can be accounted for by static coulombic-like

Table 4. Examination of Catalytic Activity of the Related Compounds

Entry	Catalyst (mol %)	Solvent	Time (hr)	Yield of 3a (%) ^a
 [2-Ph-N-MeOx]OTf [100mol% or 2mol%]				
1	BPh ₃ (100)	CD ₃ CN	12	0
2	B(C ₆ F ₅) ₃ (100)	CD ₃ CN	12	0
3	 MIDA (2 or 100)	CD ₃ CN	12	0
4	 [2-Ph-N-MeOx]OTf (100 or 2)	CD ₃ CN	12	0
5	 2-PhOx (100)	CDCl ₃	5	0  2-PhOx-HBpin (89%)
6	 N-MeOx·BPh ₃ (100 or 2)	CDCl ₃ ^b	48	12 (100 mol % of catalyst)
		CD ₃ CN	12	6 (2 mol % of catalyst)
7	 1d (2)	CD ₃ CN	0.5	97
8	 NDI (100 or 2)	CDCl ₃ ^b	12	0

Reaction conditions: acetophenone (0.269 mmol), HBpin (0.269 mmol), solvent (0.5 mL).

^aYields were determined by ¹H NMR spectroscopy.

^bBecause of the poor solubility of N-MeOx·BPh₃ and NDI in CD₃CN, the reactions were performed in CDCl₃.

interactions.^{65–67} To gain more insight into the catalytic mechanism, we further investigated the hydroboration reaction of 2a by using several related compounds as the catalysts (Table 4).

When a stoichiometric amount of BPh₃ or B(C₆F₅)₃ was used, no reactions were observed, even after 12 hr (Figures S5 and S6, entries 1 and 2), confirming that typical Lewis acids do not catalyze the hydroboration reaction under the reaction

conditions. Thus, unoccupied orbitals such as an empty p orbital on the B atom or any σ holes (σ^* orbitals)⁶⁸ seem to be irrelevant to the hydroboration reaction with **6**. Neither a catalytic amount (2 mol %) nor a stoichiometric amount of 1-methylindole-2-boronic acid MIDA ester MIDA featuring a dative N: \rightarrow B bond promoted the reaction (Figure S7, entry 3). Analogously, 2-phenyl-*N*-methyloxazolium ion [2-Ph-*N*-MeOx]OTf was not effective as the catalyst at all (Figure S8, entry 4). We also examined a combination of an oxazoline and a borane (entry 5). At first, we confirmed that no adduct was formed between 2-phenyloxazoline 2-PhOx and BPh₃ in CD₃CN. Both **2a** and HBpin were added to this solution, and the reaction was monitored by NMR spectroscopy. **2a** remained stable after 5 hr, but the hydroboration of 2-PhOx proceeded to afford 2-PhOx-HBpin cleanly (Figure S9). Thus, the Lewis pair 2-PhOx/BPh₃ does not serve as the catalyst for the hydroboration of **2a**, suggesting that the dissociation of the B–N bonds in **6** and **1c** to function as if to act as the frustrated Lewis pairs is unlikely during the hydroboration reaction of carbonyls in our system.^{69,70} Interestingly, with a stoichiometric amount of the adduct of *N*-methyloxazol-2-ylidene with BPh₃ *N*-MeOx·BPh₃ in a CDCl₃ solution, a small amount of **3a** was formed (12%) after 48 hr (Figure S10, entry 6). We confirmed that the use of a catalytic amount (2 mol %) of *N*-MeOx·BPh₃ also afforded **3a**, albeit in very low yield (6%) (Figure S11). Because no dissociation of *N*-Me·Ox·BPh₃ to the corresponding oxazol-2-ylidene and BPh₃ was observed in either a CDCl₃ or a CD₃CN solution, *N*-Me·Ox·BPh₃ is also likely to function as an electrostatic catalyst. Remarkably, we found that compound **1d** featuring a B₂C₂N₂ six-membered ring akin to those of **6** and **1c**, effectively promoted the reaction (entry 7). With 2 mol % of **1d**, nearly quantitative formation of **3a** was observed after 30 min (Figure S12). From these results, the polarized B₂C₂N₂ skeleton is putatively a key structure to enhance the catalytic activity as an electrostatic functionality. In addition, we tested a π -acidic naphthalene diimide NDI,⁷¹ known for its ability for noncovalent electrophilic activation of organic substrates as pioneered by Matile et al.,^{72,73} but no formation of **3a** was observed (Figure S13, entry 8).

Catalytic N-Formylation of Amines with CO₂

Over the past few decades, various strategies have been developed for activating thermodynamically highly stable carbon dioxide (CO₂) and achieving its subsequent transformation into commodity chemicals with both metal and nonmetal catalysts.^{74–85} Among them, N-formylation of amines with CO₂ as the carbon source has been attracting great interest because the reaction products, that is, formamides, are ubiquitous in organic syntheses as well as industrial products as synthetic intermediates and solvents.^{86–99} Previously, we showed that compound **1a** reversibly undergoes a [4 + 2] cycloaddition reaction with CO₂,⁵⁶ which prompted us to investigate further the catalytic activity of **1a** for functionalization of CO₂.

We began our investigation by using *N*-methylaniline **7a** as a test substrate for N-formylation with CO₂. After a brief screening of the reaction conditions (Table S1), we obtained the optimal conditions under which, with **1a** (2 mol %) and HBpin (3 equiv) under a CO₂ atmosphere, **7a** was transformed nearly quantitatively to *N*-methyl-*N*-phenylformamide **8a** after 5.5 hr at room temperature (Figure 4).

Next, the scope of the N-formylation reaction was studied with various amines (Table 5). Aromatic primary amines **7b–7g** were well tolerated and the corresponding formamides **8b–8g** were obtained in good to excellent yields (76%–95%). Secondary amines **7h–7n** bearing an aromatic ring with varying degrees of electronic features afforded the corresponding N-formylated products **8h–8n** in high yields (80%–98%).

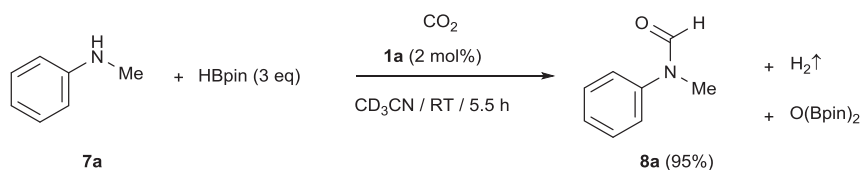


Figure 4. Catalytic N-Formylation with 1a

N-Formylation reaction of PhMeNH with CO₂ catalyzed by 1a.

We observed that dialkylamines such as diethylamine and diisopropylamine predominantly underwent dehydrocoupling with HBpin. The strong nucleophilic nature of dialkylamines probably accelerated the dehydrocoupling reaction before the N-formylation, which is in line with the recent report by Romero et al.¹⁰⁰ on the noncatalyzed dehydrocoupling reaction between amines and boranes.

Mechanistic Study and a Proposed Catalytic Cycle

To identify a plausible reaction mechanism, we performed several control reactions. In the absence of 1a, a mixture of *N*-methylaniline 7a and HBpin (3 equiv) afforded *N*-formyl-*N*-methylaniline 8a only in 5% yield even after 20 hr, confirming the essential involvement of the catalyst in the N-formylation reaction (Table S1, entry 1). Neither HBpin nor 7a reacted with 1a, suggesting that compound 10, an adduct of 1a with CO₂, must be formed in the initial step of the reaction. We confirmed that 10, independently prepared from the reaction of 1a with CO₂, did not react with 7a (Figure 5A, top). By contrast, treatment of a CD₃CN solution of 10 with HBpin (3 equiv) under an argon atmosphere produced HCOOBpin 11 as the major product along with other minor side products, including O(Bpin)₂ (Figure 5A, bottom; Figures S14 and S15). We found that with 2 mol % of 1a, hydroboration of CO₂ proceeded smoothly and 11 was formed in 48% yield after 34 hr (Figures 5B, S16, and S17). The yield of 11 increased (70%) when 9 mol % 1a was used (Figures S18 and S19). Moreover, a stoichiometric reaction of HCOOBpin 11 and 7a with HBpin (2.5 equiv) afforded *N*-formyl-*N*-methylaniline 8a quantitatively, confirming that this process does not require any catalysts (Figures 5C, S20, and S21). Interestingly, the reaction of 7a (1 equiv) with HBpin (3 equiv) in the presence of 10 furnished dehydrocoupling product PhMeNBpin 9a without formation of 8a (Figures 5D, S22, and S23). This result indicates that 10 only promotes the dehydrocoupling reaction^{101–105} in the presence of amine rather than reacting with HBpin to afford 11 (Figure 5A, bottom). In order to confirm whether dehydrocoupling product 9a is involved as the key intermediate in the catalytic cycle, 9a was reacted with HBpin under a CO₂ atmosphere (Figure 5E). Without 1a, no reaction between 9a and HBpin was observed, whereas the same reaction in the presence of 1a (2 mol %) afforded 8a in 15% yield after 7 hr (Figure S24). Although the result shows that 1a can marginally promote the formation of 8a from 9a, this reaction is much slower than that shown in Figure 4, suggesting that the reaction pathway involving a dehydrocoupling intermediate such as 9a is subordinate for N-formylation of amines. We synthesized 10-(¹³CO₂) by the treatment of 1a with ¹³CO₂, and conducted the reaction of 10-(¹³CO₂) with 7a (1 equiv) and HBpin (3 equiv) under CO₂ (Figures 5F and S25–S27). After 7 hr, we observed the formation of 8a in 95% yield, which is in stark contrast to the exclusive formation of dehydrocoupling product 9a from the reaction without CO₂ (Figure 5D). The ¹³C NMR spectrum of formamide 8a confirmed that the ¹³C atom was not incorporated in product 8a, indicating that transfer of the CO₂ fragment from 10-(¹³CO₂) to HBpin as observed in Figure 5A did not take place during the catalytic N-formylation. Thus, compound 10 is not the resting state but is a species that serves as the active catalyst in the N-formylation reaction.

Table 5. Scope of Catalytic N-Formylation of Amines with CO₂

		Time (hr)	Product 8	Yield (%) ^a	TON	TOF (hr ⁻¹)
7b		10	8b	95	48	5
7c		23	8c	81	41	2
7d		16	8d	87	44	3
7e		20	8e	94	47	2
7f		12	8f	87	44	4
7g		22	8g	76	38	2
7h		11	8h	85	43	4
7i		5.5	8i	98	49	9
7j		4	8j	93	47	12
7k		21	8k	80	40	2
7l		8	8l	94	47	6
7m		21	8m	80	40	2
7n		5	8n	83	42	8

^aYields were determined by ¹H NMR spectroscopy using 1,3,5-trimethoxybenzene as an internal standard.

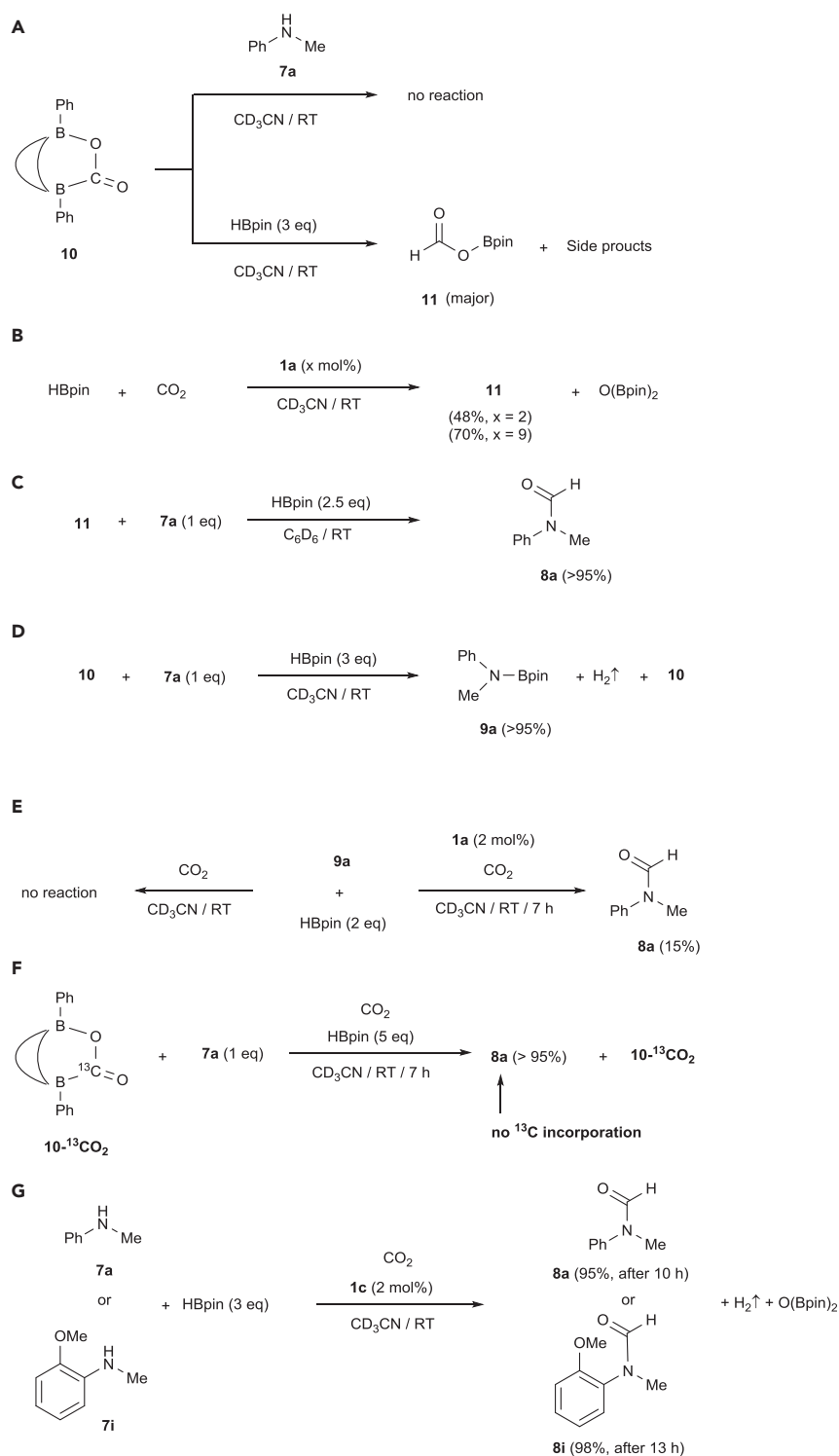


Figure 5. Control Reactions for Mechanistic Studies

(A) Reactions of **10** with **7a** (top) and HBpin (bottom).

(B) Catalytic hydroboration of CO₂ using **1a**.

(C) Synthesis of **8a** from **1a** and **7a**.

Figure 5. Continued

- (D) Reaction of **7a** and HBpin in the presence of **10**.
 (E) Reactions of **9a** and HBpin, with and without **1a** under CO₂.
 (F) Reaction of **10**-(¹³CO₂), **7a**, and HBpin under CO₂.
 (G) Catalytic hydroboration of CO₂ using **1c**.

A series of recent seminal works^{106–108} demonstrated that the formaldehyde adducts¹⁰⁹ of ambiphilic phosphine-borane catalysts were generated in catalytic hydroboration of CO₂, and the CH₂O moiety remained in the ambiphilic system throughout the catalysis. Thus, it is postulated that the formaldehyde adducts are active catalysts in their catalytic hydroboration reaction. On the basis of the outcomes of our control reactions (Figure 5), it is well conceivable that CO₂-adduct **10** could also serve as the catalyst, which was confirmed by DFT calculations (Figure S49). Accordingly, one of the most plausible reaction mechanisms is proposed in Figure 6. At the initial stage of the reaction, compound **10** is formed in situ after the reaction of **1a** with CO₂. Compound **10** can activate the B–H bond of HBpin, which is followed by transfer of the hydride to CO₂ to furnish HCOOBpin **11**, concomitant with regeneration of **10**. The activation barrier (18.8 kcal mol^{−1}) of this process is lower than that (40.1 kcal mol^{−1}) of another path involving the transition state stabilized by an electrostatic interaction of **10** (Figure S49). The non-catalytic reaction between **11** and amines **7** should produce formamides **8** as well as HOBpin, which can undergo dehydrocoupling with HBpin to form O(Bpin)₂. Note that although a number of reaction mechanisms have been proposed for the p-block compound-catalyzed hydroboration of CO₂^{34,110–114} and/or N-formylation of amines with CO₂,^{92–99} to the best of our knowledge, none of these studies has assumed that main-group compound-CO₂ adducts play a role as the actual active catalysts.

Analogous N-formylation could take place when **1c** was used as the catalyst. Thus, under similar reaction conditions, amines **7a** and **7i** were cleanly transformed to the corresponding formamides **8a** and **8i**, respectively (Figure 5G). Experimentally, we confirmed that **1c** cannot be converted to **10** in a CD₃CN solution under a CO₂ atmosphere (Figures S35 and S36). Because **1c** does not possess a strong Lewis basic site akin to the O=C=O moiety of **10** to activate HBpin, on the basis of the

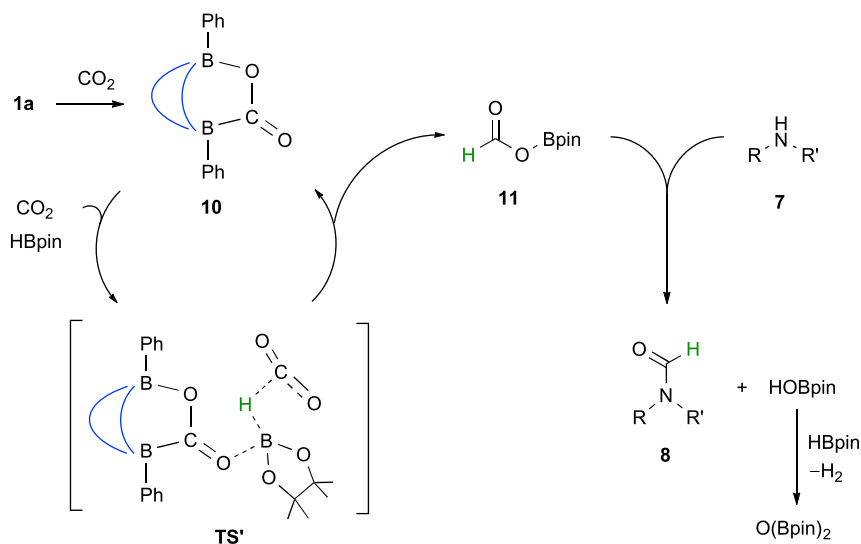


Figure 6. Proposed Reaction Mechanism

Plausible catalytic cycle for the N-formylation of amines with HBpin under CO₂.

above-mentioned results for the catalytic hydroboration of ketones (**2a** and **2h**) with **1c**, we tentatively postulate that **1c** could act as an electrostatic catalyst for the formation of formamides (**8a** and **8i**).

Conclusions

We have demonstrated that a catalytic amount of inorganic/organic hybrid benzene, 1,3,2,5-diazadiborinine **1a**, effectively promotes hydroboration of carbonyl derivatives involving ketones, aldehydes, and CO₂ under metal-free and ambient conditions. Mechanistic studies suggest that the corresponding carbonyl adducts **6** and **10** are formed in the initial steps of those reactions. Significantly, neither of the catalytic cycles seems to involve the regeneration of **1a**, and thus, adducts **6** and **10** serve as the actual active catalysts rather than the resting states, which is in contrast to the proposed mechanisms for other main-group compound-catalyzed reduction of carbonyl derivatives. Computational studies suggest that among various possible factors, a noncovalent interaction plays a critical role in facilitating some of the reactions examined here. Thus, the electrostatic effect induced by the polar and hole-shaped structures of the carbonyl adduct **6** helps decrease the activation barrier for the hydroboration reactions of ketones and aldehydes. In contrast, the CO₂-adduct **10** serves as a Lewis base to activate the B–H bond of HBpin during the reduction of CO₂. We believe that the findings described here pave the way for the design of novel nonmetal p-block catalysts.

EXPERIMENTAL PROCEDURES

Full experimental procedures are provided in the [Supplemental Information](#).

ACCESSION NUMBERS

Crystallographic data have been deposited in the Cambridge Crystallographic Data Center (CCDC) under accession number CCDC: 1523108. The data can be obtained free of charge from the CCDC at http://www.ccdc.cam.ac.uk/data_request/cif.

SUPPLEMENTAL INFORMATION

Supplemental Information includes Supplemental Experimental Procedures, 166 figures, 4 tables, and 1 data file and can be found with this article online at <http://dx.doi.org/10.1016/j.chempr.2017.06.001>.

AUTHOR CONTRIBUTIONS

D.W. performed the synthetic studies. Y.L. and R.G. conducted single-crystal X-ray diffraction studies. R.W. and H.H. performed the computational experiments. R.K. directed the project and wrote the manuscript with input from all authors. All authors analyzed the results and commented on the manuscript.

ACKNOWLEDGMENTS

We are grateful to Nanyang Technological University (NTU) and the Singapore Ministry of Education (MOE2015-T2-2-032) for financial support. H.H. acknowledges financial support from City University of Hong Kong (CityU; 7200534 and 9610369) and the supercomputer resources at NTU, CityU, and Hong Kong Baptist University.

Received: December 30, 2016

Revised: February 7, 2017

Accepted: June 5, 2017

Published: July 13, 2017

REFERENCES AND NOTES

- Mahadevi, A.S., and Sastry, G.N. (2016). Cooperativity in noncovalent interactions. *Chem. Rev.* 116, 2775–2825.
- Maharramov, A.M., Mahmudov, K.T., Kopylovich, M.N., and Pombeiro, A.J.L. (2016). Non-Covalent Interactions in the Synthesis and Design of New Compounds (John Wiley).
- Baev, A.K. (2012). Specific Intermolecular Interactions of Organic Compounds (Springer).
- Baev, A.K. (2014). Specific Intermolecular Interactions of Nitrogenated and Bioorganic Compounds (Springer).
- Hobza, P., and Müller-Dethlefs, K. (2010). Non-Covalent Interactions: Theory and Experiment (Royal Society of Chemistry).
- Hanoian, P., Liu, C.T., Hammes-Schiffer, S., and Benkovic, S. (2015). Perspectives on electrostatics and conformational motions in enzyme catalysis. *Acc. Chem. Res.* 48, 482–489.
- Herschlag, D., and Natarajan, A. (2013). Fundamental challenges in mechanistic enzymology: progress toward understanding the rate enhancements of enzymes. *Biochemistry* 52, 2050–2067.
- Warshel, A., Sharma, P.K., Kato, M., Xiang, Y., Liu, H., and Olsson, M.H.M. (2006). Electrostatic basis for enzyme catalysis. *Chem. Rev.* 106, 3210–3235.
- Jeffrey, G.A. (1997). An Introduction to Hydrogen Bonding (Oxford University Press).
- Desiraju, G.R., and Steiner, T. (1999). The Weak Hydrogen Bond in Structural Chemistry and Biology (Oxford University Press).
- Pihko, P.M. (2009). Hydrogen Bonding in Organic Synthesis (Wiley-VCH).
- Gilli, G., and Gilli, P. (2009). The Nature of the Hydrogen Bond (Oxford University Press).
- Sohtome, Y., and Nagasawa, K. (2012). Dynamic asymmetric organocatalysis: cooperative effects of weak interactions and conformational flexibility in asymmetric organocatalysts. *Chem. Commun.* 48, 7777–7789.
- Fu, X., and Tan, C.-H. (2011). Mechanistic considerations of guanidine-catalyzed reactions. *Chem. Commun.* 47, 8210–8222.
- Mahmudov, K.T., Kopylovich, M.N., Silva, M.F.C.G.d., and Pombeiro, A.J.L. (2016). Non-covalent interactions in the synthesis of coordination compounds: recent advances. *Coord. Chem. Rev.* <http://dx.doi.org/10.1016/j.ccr.2016.09.002>.
- Scheiner, S. (2015). Noncovalent Forces (Springer).
- Giese, M., Albrecht, M., and Rissanen, K. (2015). Anion- π interactions with fluoroarenes. *Chem. Rev.* 115, 8867–8895.
- Metrangolo, P., and Resnati, G. (2010). Halogen Bonding: Fundamentals and Applications (Structure and Bonding) (Springer).
- Ma, J.C., and Dougherty, D.A. (1997). The cation- π interaction. *Chem. Rev.* 97, 1303–1324.
- Zaidlewicz, M., and Pakulski, M.M. (2011). Reduction of carbonyl groups: transfer hydrogenation, hydrosilylation, catalytic hydroboration, and reduction with borohydrides, aluminum hydrides, or boranes. In *Science of Synthesis, Stereoselective Synthesis*, Vol. 2, J.G. De Vries, G.A. Molander, and P.A. Evans, eds. (Georg Thieme Verlag), pp. 59–131.
- Abdel-Magid, A.F. (1998). Reductions in Organic Synthesis. Recent Advances and Practical Applications; ACS Symposium Series (American Chemical Society).
- Hudlicky, M. (1984). Reductions in Organic Chemistry (John Wiley).
- Magano, J., and Dunetz, J.R. (2012). Large-scale carbonyl reductions in the pharmaceutical industry. *Org. Process Res. Dev.* 16, 1156–1184.
- Burkhardt, E.R., and Matos, K. (2006). Boron reagents in process chemistry: excellent tools for selective reductions. *Chem. Rev.* 106, 2617–2650.
- Arai, N., and Ohkuma, T. (2011). Reduction of carbonyl groups: hydrogenation. In *Science of Synthesis, Stereoselective Synthesis*, Vol. 2, J.G. De Vries, G.A. Molander, and P.A. Evans, eds. (Georg Thieme Verlag), pp. 9–57.
- Cho, B.T. (2009). Recent development and improvement for boron hydride-based catalytic asymmetric reduction of unsymmetrical ketones. *Chem. Soc. Rev.* 38, 443–452.
- Andersson, P.G., and Munslow, I.J. (2008). Modern Reduction Methods (Wiley-VCH).
- Togni, A., and Grützmacher, H. (2001). Catalytic Heterofunctionalization: from Hydroamination to Hydrozirconation (Wiley-VCH).
- Hayashi, T. (1999). Hydroboration of Carbon-Carbon Double Bonds. In *Comprehensive Asymmetric Catalysis*, Vol. 1, E.N. Jacobsen, A. Pfaltz, and H. Yamamoto, eds. (Springer), pp. 351–366.
- Beletskaya, I., and Pelter, A. (1997). Hydroborations catalysed by transition metal complexes. *Tetrahedron* 53, 4957–5026.
- Lennox, A.J.J., and Lloyd-Jones, G.C. (2014). Selection of boron reagents for Suzuki–Miyaura coupling. *Chem. Soc. Rev.* 43, 412–443.
- Hartwig, J.F. (2012). Borylation and silylation of C–H bonds: a platform for diverse C–H bond functionalizations. *Acc. Chem. Res.* 45, 864–873.
- Soloway, A.H., Tjarks, W., Barnum, B.A., Rong, F.-G., Barth, R.F., Codogni, I.M., and Wilson, J.G. (1998). The chemistry of neutron capture therapy. *Chem. Rev.* 98, 1515–1562.
- Chong, C.C., and Kinjo, R. (2015). Catalytic hydroboration of carbonyl derivatives, imines, and carbon dioxide. *ACS Catal.* 5, 3238–3259.
- Stephan, D.W., and Erker, G. (2015). Frustrated Lewis pair chemistry: development and perspectives. *Angew. Chem. Int. Ed.* 54, 6400–6441.
- Martin, D., Soleilhavoup, M., and Bertrand, G. (2011). Stable singlet carbenes as mimics for transition metal centers. *Chem. Sci.* 2, 389–399.
- Power, P.P. (2010). Main-group elements as transition metals. *Nature* 463, 171–177.
- Blake, A.J., Cunningham, A., Ford, A., Teat, S.J., and Woodward, S. (2000). Enantioselective reduction of prochiral ketones by catecholborane catalysed by chiral group 13 complexes. *Chem. Eur. J.* 6, 3586–3594.
- Ford, A., and Woodward, S. (1999). Catalytic enantioselective reduction of ketones by a chiral gallium complex and catecholborane. *Angew. Chem. Int. Ed.* 38, 335–336.
- Arrowsmith, M., Hadlington, T.J., Hill, M.S., and Kociok-Köhn, G. (2012). Magnesium-catalysed hydroboration of aldehydes and ketones. *Chem. Commun.* 48, 4567–4569.
- Weetman, C., Anker, M.D., Arrowsmith, M., Hill, M.S., Kociok-Köhn, G., Liprott, D.J., and Mahon, M.F. (2016). Magnesium-catalysed nitrile hydroboration. *Chem. Sci.* 7, 628–641.
- Intemann, J., Lutz, M., and Harder, S. (2014). Multinuclear magnesium hydride clusters: selective reduction and catalytic hydroboration of pyridines. *Organometallics* 33, 5722–5729.
- Arrowsmith, M., Hill, M.S., and Kociok-Köhn, G. (2013). Magnesium catalysis of imine hydroboration. *Chem. Eur. J.* 19, 2776–2783.
- Arrowsmith, M., Hill, M.S., Hadlington, T., Kociok-Köhn, G., and Weetman, C. (2011). Magnesium-catalyzed hydroboration of pyridines. *Organometallics* 30, 5556–5559.
- Fohlmeister, L., and Stasch, A. (2016). Ring-shaped phosphinoamido-magnesium-hydride complexes: syntheses, structures, reactivity, and catalysis. *Chem. Eur. J.* 22, 10235–10246.
- Hadlington, T.J., Hermann, M., Frenking, G., and Jones, C. (2014). Low coordinate germanium(II) and tin(II) hydride complexes: efficient catalysts for the hydroboration of carbonyl compounds. *J. Am. Chem. Soc.* 136, 3028–3031.
- Hadlington, T.J., Hermann, M., Frenking, G., and Jones, C. (2015). Two-coordinate group 14 element(II) hydrides as reagents for the facile, and sometimes reversible, hydrogermylation/hydrostannylation of unactivated alkenes and alkynes. *Chem. Sci.* 6, 7249–7257.
- Hadlington, T.J., Schwarze, B., Izgorodina, E.I., and Jones, C. (2015). Two-coordinate hydrido-germylenes. *Chem. Commun.* 51, 6854–6857.

49. Hadlington, T.J., and Jones, C. (2014). A singly bonded amido-distannyne: H₂ activation and isocyanide coordination. *Chem. Commun.* 50, 2321–2323.
50. Hadlington, T.J., Hermann, M., Li, J., Frenking, G., and Jones, C. (2013). Activation of H₂ by a multiply bonded amido-digermine: evidence for the formation of a hydrido-germylene. *Angew. Chem. Int. Ed.* 52, 10199–10203.
51. Yang, Z., Zhong, M., Ma, X., De, S., Anusha, C., Parameswaran, P., and Roesky, H.W. (2015). An aluminum hydride that functions like a transition-metal catalyst. *Angew. Chem. Int. Ed.* 54, 10225–10229.
52. Jakhar, V.K., Barman, M.K., and Nembenna, S. (2016). Aluminum monohydride catalyzed selective hydroboration of carbonyl compounds. *Org. Lett.* 18, 4710–4713.
53. Mukherjee, D., Osseili, H., Spaniol, T.P., and Okuda, J. (2016). Alkali metal hydridotriphenylborates [LJM][HBPh₃] (M = Li, Na, K): chemoselective catalysts for carbonyl and CO₂ hydroboration. *J. Am. Chem. Soc.* 138, 10790–10793.
54. Chong, C.C., Hirao, H., and Kinjo, R. (2015). Metal-free σ -bond metathesis in 1,3,2-diazaphospholene-catalyzed hydroboration of carbonyl compounds. *Angew. Chem. Int. Ed.* 54, 190–194.
55. Wu, D., Ganguly, R., Li, Y., Hoo, S.N., Hirao, H., and Kinjo, R. (2015). Reversible [4 + 2] cycloaddition reaction of 1,3,2,5-diazadiborinine with ethylene. *Chem. Sci.* 6, 7150–7155.
56. Wu, D., Kong, L., Li, Y., Ganguly, R., and Kinjo, R. (2015). 1,3,2,5-Diazadiborinine featuring nucleophilic and electrophilic boron centres. *Nat. Commun.* 6, 7340.
57. Wang, B., Li, Y., Ganguly, R., Hirao, H., and Kinjo, R. (2016). Ambiphilic boron in 1,4,2,5-diazadiborinine. *Nat. Commun.* 7, 11871.
58. Wang, X.-Y., Wang, J.-Y., and Pei, J. (2015). BN heterosuperbenzenes: synthesis and properties. *Chem. Eur. J.* 21, 3528–3529.
59. Campbell, P.G., Marwitz, A.J.V., and Liu, S.-Y. (2012). Recent advances in azaborine chemistry. *Angew. Chem. Int. Ed.* 51, 6074–6092.
60. Bosdet, M.J.D., and Piers, W.E. (2008). B–N as a C–C substitute in aromatic systems. *Can. J. Chem.* 86, 8–29.
61. Longobardi, L.E., Russell, C.A., Green, M., Townsend, N.S., Wang, K., Holmes, A.J., Duckett, S.B., McGrady, J.E., and Stephan, D.W. (2014). Hydrogen activation by an aromatic triphosphabenzene. *J. Am. Chem. Soc.* 136, 13453–13457.
62. Tsao, F.A., Cao, L., Grimme, S., and Stephan, D.W. (2015). Double FLP-alkyne exchange reactions: a facile route to Te/B heterocycles. *J. Am. Chem. Soc.* 137, 13264–13267.
63. Angeles-Boza, A.M., Ertem, M.Z., Sarma, R., Ibañez, C.H., Maji, S., Llobet, A., Cramer, C.J., and Roth, J.P. (2014). Competitive oxygen-18 kinetic isotope effects expose O–O bond formation in water oxidation catalysis by monomeric and dimeric ruthenium complexes. *Chem. Sci.* 5, 1141–1152.
64. Angeles-Boza, A.M., and Roth, J.P. (2012). Oxygen kinetic isotope effects upon catalytic water oxidation by a monomeric ruthenium complex. *Inorg. Chem.* 51, 4722–4729.
65. von Hopffgarten, M., and Frenking, G. (2012). Energy decomposition analysis. *Wires Comput. Mol. Sci.* 2, 43–62.
66. Hirao, H. (2007). Reactive bond orbitals: a localized resonance-structure approach to charge transfer. *Chem. Phys. Lett.* 443, 141–146.
67. Kitaura, K., and Morokuma, K. (1976). A new energy decomposition scheme for molecular interactions within the Hartree-Fock approximation. *Int. J. Quant. Chem.* 10, 325–340.
68. Benz, S., López-Andarias, J., Mareda, J., Sakai, N., and Matile, S. (2017). Catalysis with chalcogen bonds. *Angew. Chem. Int. Ed.* 56, 812–815.
69. Our system differs from the Corey-Bakshi-Shibata system, which is historically the first example of carbonyl hydroboration catalyzed by an ambiphilic boron heterocycle. See Corey et al.⁷⁰
70. Corey, E.J., Bakshi, R.K., and Shibata, S. (1987). Highly enantioselective borane reduction of ketones catalyzed by chiral oxazaborolidines. Mechanism and synthetic implications. *J. Am. Chem. Soc.* 109, 5551–5553.
71. Kobaisi, K.A., Bhosale, S.V., Latham, K., Raynor, A.M., and Bhosale, S.V. (2016). Functional naphthalene diimides: synthesis, properties, and applications. *Chem. Rev.* 116, 11685–11796.
72. Dawson, R.E., Hennig, A., Weimann, D.P., Emery, D., Ravikumar, V., Montenegro, J., Takeuchi, T., Gabutti, S., Mayor, M., Mareda, J., et al. (2010). Experimental evidence for the functional relevance of anion- π interactions. *Nat. Chem.* 2, 533–538.
73. Zhao, Y., Domoto, Y., Orentas, E., Beuchat, C., Emery, D., Mareda, J., Sakai, N., and Matile, S. (2013). Catalysis with anion- π interactions. *Angew. Chem. Int. Ed.* 52, 9940–9943.
74. Liu, Q., Wu, L., Jackstell, R., and Beller, M. (2015). Using carbon dioxide as a building block in organic synthesis. *Nat. Commun.* 6, 5933.
75. Tlili, A., Blondiaux, E., Frogneux, X., and Cantat, T. (2015). Reductive functionalization of CO₂ with amines: an entry to formamide, formamidine and methylamine derivatives. *Green Chem.* 17, 157–168.
76. Yeung, C.S., and Dong, V.M. (2014). Making C–C bonds from carbon dioxide via transition-metal catalysis. *Top. Catal.* 57, 1342–1350.
77. Maeda, C., Miyazaki, Y., and Ema, T. (2014). Recent progress in catalytic conversions of carbon dioxide. *Catal. Sci. Technol.* 4, 1482–1497.
78. Aresta, M., Dibenedetto, A., and Angelini, A. (2014). Catalysis for the valorization of exhaust carbon: from CO₂ to chemicals, materials, and fuels. Technological use of CO₂. *Chem. Rev.* 114, 1709–1742.
79. Appel, A.M., Bercaw, J.E., Bocarsly, A.B., Dobbek, H., DuBois, D.L., Dupuis, M., Ferry, J.G., Fujita, E., Hille, R., Kenis, P.J.A., et al. (2013). Frontiers, opportunities, and challenges in biochemical and chemical catalysis of CO₂ fixation. *Chem. Rev.* 113, 6621–6658.
80. Lu, X.-B., Ren, W.-M., and Wu, G.-P. (2012). CO₂ copolymers from epoxides: catalyst activity, product selectivity, and stereochemistry control. *Acc. Chem. Res.* 45, 1721–1735.
81. Lu, X.-B., and Darensbourg, D.J. (2012). Cobalt catalysts for the coupling of CO₂ and epoxides to provide polycarbonates and cyclic carbonates. *Chem. Soc. Rev.* 41, 1462–1484.
82. Omae, I. (2012). Recent developments in carbon dioxide utilization for the production of organic chemicals. *Coord. Chem. Rev.* 256, 1384–1405.
83. Cokoja, M., Bruckmeier, C., Rieger, B., Herrmann, W.A., and Kühn, F.E. (2011). Transformation of carbon dioxide with homogeneous transition-metal catalysts: a molecular solution to a global challenge? *Angew. Chem. Int. Ed.* 50, 8510–8537.
84. Riduan, S.N., and Zhang, Y. (2010). Recent developments in carbon dioxide utilization under mild conditions. *Dalton Trans.* 39, 3347–3357.
85. Sakakura, T., Choi, J.-C., and Yasuda, H. (2007). Transformation of carbon dioxide. *Chem. Rev.* 107, 2365–2387.
86. Nguyen, T.V.Q., Yoo, W.-J., and Kobayashi, S. (2015). Effective formylation of amines with carbon dioxide and diphenylsilane catalyzed by chelating bis(tzNHC) rhodium complexes. *Angew. Chem. Int. Ed.* 54, 9209–9212.
87. Motokura, K., Takahashi, N., Miyaji, A., Sakamoto, Y., Yama-guchi, S., and Baba, T. (2014). Mechanistic studies on the N-formylation of amines with CO₂ and hydrosilane catalyzed by a Cu-diphosphine complex. *Tetrahedron* 70, 6951–6956.
88. Frogneux, X., Jacquet, O., and Cantat, T. (2014). Iron-catalyzed hydrosilylation of CO₂: CO₂ conversion to formamides and methylamines. *Catal. Sci. Technol.* 4, 1529–1533.
89. González-Sebastián, L., Flores-Alamo, M., and Garcia, J.J. (2013). Nickel-catalyzed hydrosilylation of CO₂ in the presence of Et₃B for the synthesis of formic acid and related formates. *Organometallics* 32, 7186–7194.
90. Itagaki, S., Yamaguchi, K., and Mizuno, N. (2013). Catalytic synthesis of silyl formates with 1 atm of CO₂ and their utilization for synthesis of formyl compounds and formic acid. *J. Mol. A Chem.* 366, 347–352.
91. Motokura, K., Takahashi, N., Kashiwame, D., Yamaguchi, S., Miyaji, A., and Baba, T. (2013). Copper-diphosphine complex catalysts for N-formylation of amines under 1 atm

- of carbon dioxide with polymethylhydrosiloxane. *Catal. Sci. Technol.* **3**, 2392–2396.
92. Das, S., Bobbink, F.D., Bulut, S., Soudani, M., and Dyson, P.J. (2016). Thiazolium carbene catalysts for the fixation of CO₂ onto amines. *Chem. Commun.* **52**, 2497–2500.
93. Chong, C.C., and Kinjo, R. (2015). Hydrophosphination of CO₂ and subsequent formate transfer in the 1,3,2-diazaphospholene-catalyzed N-formylation of amines. *Angew. Chem. Int. Ed.* **54**, 12116–12120.
94. Frogneux, X., Blondiaux, E., Thuéry, P., and Cantat, T. (2015). Bridging amines with CO₂: organocatalyzed reduction of CO₂ to amins. *ACS Catal.* **5**, 3983–3987.
95. Zhou, H., Wang, G.-X., Zhang, W.-Z., and Lu, X.-B. (2015). CO₂ adducts of phosphorus ylides: highly active organocatalysts for carbon dioxide transformation. *ACS Catal.* **5**, 6773–6779.
96. Hao, L., Zhao, Y., Yu, B., Yang, Z., Zhang, H., Han, B., Gao, X., and Liu, Z. (2015). Imidazolium-based ionic liquids catalyzed formylation of amines using carbon dioxide and phenylsilane at room temperature. *ACS Catal.* **5**, 4989–4993.
97. Blondiaux, E., Pouessel, J., and Cantat, T. (2014). Carbon dioxide reduction to methylamines under metal-free conditions. *Angew. Chem. Int. Ed.* **53**, 12186–12190.
98. Gomes, C.D.N., Jacquet, O., Villiers, C., Thuéry, P., Ephri-tikhine, M., and Cantat, T. (2012). A diagonal approach to chemical recycling of carbon dioxide: organocatalytic transformation for the reductive functionalization of CO₂. *Angew. Chem. Int. Ed.* **51**, 187–190.
99. Jacquet, O., Gomes, C.D.N., Ephritikhine, M., and Cantat, T. (2012). Recycling of carbon and silicon wastes: room temperature formylation of N–H bonds using carbon dioxide and polymethylhydrosiloxane. *J. Am. Chem. Soc.* **134**, 2934–2937.
100. Romero, E.A., Peltier, J.L., Jazara, R., and Bertrand, G. (2016). Catalyst-free dehydrocoupling of amines, alcohols, and thiols with pinacol borane and 9-borabicyclononane (9-BBN). *Chem. Commun.* **52**, 10563–10565.
101. Harinath, A., Anga, S., and Panda, T.K. (2016). Alkali metal catalyzed dehydro-coupling of boranes and amines leading to the formation of a B–N bond. *RSC Adv.* **6**, 35648–35653.
102. Yang, Z., Zhong, M., Ma, X., Nijesh, K., De, S., Parameswaran, P., and Roesky, H.W. (2016). An aluminum dihydride working as a catalyst in hydroboration and dehydrocoupling. *J. Am. Chem. Soc.* **138**, 2548–2551.
103. Bolaño, T., Esteruelas, M.A., Gay, M.P., Oñate, E., Pastor, I.M., and Yus, M. (2015). An acyl-NHC osmium cooperative system: coordination of small molecules and heterolytic B–H and O–H bond activation. *Organometallics* **34**, 3902–3908.
104. Liptrot, D.J., Hill, M.S., Mahon, M.F., and Wilson, A.S.S. (2015). Alkaline-earth-catalyzed dehydrocoupling of amines and boranes. *Angew. Chem. Int. Ed.* **54**, 13362–13365.
105. Fernández-Salas, J.A., Manzini, S., and Nolan, S.P. (2013). Efficient ruthenium-catalysed S–S, S–Si and S–B bond forming reactions. *Chem. Commun.* **49**, 5829–5831.
106. Declercq, R., Bouhadir, G., Bourissou, D., Légaré, M.-A., Cour-temanche, M.-A., Nahi, K.S., Bouchard, N., Fontaine, F.-G., and Maron, L. (2015). Hydroboration of carbon dioxide using ambiphilic phosphine–borane catalysts: on the role of the formaldehyde adduct. *ACS Catal.* **5**, 2513–2520.
107. Courtemanche, M.-A., Légaré, M.-A., Maron, L., and Fontaine, F.-G. (2014). Reducing CO₂ to methanol using frustrated Lewis pairs: on the mechanism of phosphine–borane-mediated hydroboration of CO₂. *J. Am. Chem. Soc.* **136**, 10708–10717.
108. Courtemanche, M.-A., Légaré, M.-A., Maron, L., and Fontaine, F.-G. (2013). A highly active phosphine–borane organocatalyst for the reduction of CO₂ to methanol using hydroboranes. *J. Am. Chem. Soc.* **135**, 9326–9329.
109. Bontemps, S., and Sabo-Etienne, S. (2013). Trapping formaldehyde in the homogeneous catalytic reduction of carbon dioxide. *Angew. Chem. Int. Ed.* **52**, 10253–10255.
110. Bontemps, S. (2016). Boron-mediated activation of carbon dioxide. *Coord. Chem. Rev.* **308**, 117–130.
111. Fontaine, F.-G., Courtemanche, M.-A., and Légaré, M.-A. (2014). Transition-metal-free catalytic reduction of carbon dioxide. *Chem. Eur. J.* **20**, 2990–2996.
112. Wolff, N.v., Lefèvre, G., Berthet, J.-C., Thuéry, P., and Cantat, T. (2016). Implications of CO₂ activation by frustrated Lewis pairs in the catalytic hydroboration of CO₂: a view using N/Si+ frustrated Lewis pairs. *ACS Catal.* **6**, 4526–4535.
113. Tlili, A., Voituriez, A., Marinetti, A., Thuéry, P., and Cantat, T. (2016). Synergistic effects in ambiphilic phosphino-borane catalysts for the hydroboration of CO₂. *Chem. Commun.* **52**, 7553–7555.
114. Lafage, M., Pujol, A., Saffon-Merceron, N., and Mézailles, N. (2016). BH₃ activation by phosphorus-stabilized geminal dianions: synthesis of ambiphilic organoborane, DFT studies, and catalytic CO₂ reduction into methanol derivatives. *ACS Catal.* **6**, 3030–3035.